Rational design to control the trade-off between receptor affinity and cooperativity

Gabriel Ortega[a,b], Davide Mariottini[c], Alessandra Troina[c], Frederick W. Dahlquist[a,d], Francesco Ricci[c], and Kevin W. Plaxco[a,b,1]

[a]Department of Chemistry and Biochemistry, University of California, Santa Barbara, CA 93106; [b]Center for Bioengineering, University of California, Santa Barbara, CA 93106; [c]Department of Chemistry, University of Rome Tor Vergata, 00173 Rome, Italy; and [d]Department of Molecular, Cellular, and Developmental Biology, University of California, Santa Barbara, CA 93106

Edited by S. Walter Englander, Perelman School of Medicine, University of Pennsylvania, Philadelphia, PA, and approved June 20, 2020 (received for review April 12, 2020)

Cooperativity enhances the responsiveness of biomolecular receptors to small changes in the concentration of their target ligand, albeit with a concomitant reduction in affinity. The binding midpoint of a two-site receptor with a Hill coefficient of 1.9, for example, must be at least 19 times higher than the dissociation constant of the higher affinity of its two binding sites. This trade-off can be overcome, however, by the extra binding energy provided by the addition of more binding sites, which can be used to achieve highly cooperative receptors that still retain high affinity. Exploring this experimentally, we have employed an "intrinsic disorder" mechanism to design two cooperative, three-binding-site receptors starting from a single-site—and thus noncooperative—doxorubicin-binding aptamer. The first receptor follows a binding energy landscape that partitions the energy provided by the additional binding event to favor affinity, achieving a Hill coefficient of 1.9 but affinity within a factor of 2 of the parent aptamer. The binding energy landscape of the second receptor, in contrast, partitions more of this energy toward cooperativity, achieving a Hill coefficient of 2.3, but at the cost of 4-fold poorer affinity than that of the parent aptamer. The switch between these two behaviors is driven primarily by the affinity of the receptors' second binding event, which serves as an allosteric "gatekeeper" defining the extent to which the system is weighted toward higher cooperativity or higher affinity.

cooperativity | allostery | intrinsic disorder | aptamers | biosensors

Cooperativity is a property by which biomolecules achieve a steeper, more "all-or-none" response to changes in the concentration of their target ligand. Biology employs this effect in a wide range of processes, including not only the "historic" example of oxygen binding to hemoglobin, but also in the regulation of metabolism (1–4), ion transport (5, 6), neurotransmitter reuptake (7), transcription (8, 9), and translation (10). Appreciating the widespread utilization of cooperativity to improve the sensitivity of naturally occurring receptors to small changes in ligand concentration, we have recently noted that this property could also be of utility in biotechnologies, where it can be used to improve, for example, the precision with which biosensors measure small changes in the concentration of their target (11, 12).

Cooperativity (i.e., positive, homotropic allostery) occurs when a higher-affinity site on a multisite receptor binds its target only after a binding site with lower affinity for the same ligand is already occupied. Both natural (13) and artificial (11, 12, 14) systems achieve this effect by coupling the first binding event to a structural rearrangement that enhances the affinity of following binding events, leading to a higher-order dependence on ligand concentration first described by Hill over a century ago (in a single-author paper that, notably, he published while still an undergraduate) (15) before being later described in more mechanistic terms (16–18):

$$\theta = \frac{[L]^{n_H}}{[L]^{n_H} + K_{1/2}^{n_H}}. \quad [1]$$

Here, the fraction of receptors that are occupied (θ) is determined by the concentration of ligand ($[L]$), the concentration of ligand at which half of the receptors are occupied ($K_{1/2}$, which for a single binding site corresponds to the dissociation constant, K_d), and the Hill coefficient (n_H), which is a measure of the degree of cooperativity. Specifically, while a noncooperative receptor exhibits a Hill coefficient of 1, as the cooperativity increases the Hill coefficient asymptotically approaches the number of binding sites.

The cooperativity of a receptor (i.e., the magnitude of the Hill coefficient) determines the steepness of its binding curve, and thus the narrowness of its useful dynamic range (defined here as the span of ligand concentrations over which receptor occupancy varies from 10 to 90%). Specifically, the width of the dynamic range goes as follows (19):

$$\text{Dynamic Range} = 81^{1/n_H}. \quad [2]$$

The dynamic range thus transitions from 81-fold at a Hill coefficient of 1, through 9-fold at a Hill coefficient of 2, down to 3-fold when the Hill coefficient reaches 4.

Although cooperativity improves a receptor's responsiveness to small changes in ligand concentration, this useful property is not achieved without cost: it necessarily reduces the overall affinity relative to that of an equivalent noncooperative receptor. That

Significance

Cooperative binding is a property by which biomolecular receptors bind multiple-copy molecules of their targets in a highly concerted fashion, improving their responsiveness to small changes in target concentration. This mechanism is ubiquitous in the cell, where it is used to improve transport efficiency, tighten metabolic regulation, and enhance responsiveness to molecular cues. As it often happens in nature, however, this improved responsiveness comes at a cost, inevitably leading to decreased affinity. In our paper, however, we show how the additional binding energy provided by adding new binding sites can be rationally partitioned between improving the responsiveness still further or recovering some of the lost affinity, allowing the design of receptors with highly tailored affinity and cooperativity.

Author contributions: G.O., F.R., and K.W.P. designed research; G.O., D.M., and A.T. performed research; G.O., D.M., F.W.D., and K.W.P. analyzed data; and G.O. and K.W.P. wrote the paper.

The authors declare no competing interest.

This article is a PNAS Direct Submission.

Data deposition: All materials, protocols, data, models, and parameters reported in this paper have been deposited in the GitHub repository (https://github.com/gabodabo/Cooperativity-affinity-trade-off-PNAS2020).

See online for related content such as Commentaries.

[1]To whom correspondence may be addressed. Email: kwp@chem.ucsb.edu.

This article contains supporting information online at https://www.pnas.org/lookup/suppl/doi:10.1073/pnas.2006254117/-/DCSupplemental.

First published July 29, 2020.

is, because the first binding event must be of poorer affinity than at least some of the subsequent binding events, the overall affinity of the system must be poorer than the affinity of its highest-affinity site. Put more quantitatively, the overall affinity ($K_{1/2}$, the midpoint of the binding curve) of a cooperative receptor with n binding sites goes approximately as the geometric mean of the affinities of the individual binding events ($K_{d,i}$) (19):

$$K_{1/2} = \left[\prod_{i=1}^{n} K_{d,i}\right]^{1/n}. \quad [3]$$

This occurs because the overall binding free energy is given by arithmetic average of the individual binding free energies, ΔG_b:

$$\Delta G_b = {}^{1}/_{n}\left[\sum_{i=1}^{n} \Delta G_{b,i}\right] = \frac{RT}{n}\left[\sum_{i=1}^{n} \ln(K_{d,i})\right]. \quad [4]$$

For the specific example of a cooperative, two-site receptor the Hill coefficient is related to the ratio of the affinities for each site (19):

$$n_H = \frac{2}{1+\sqrt{K_{d,2}/K_{d,1}}}. \quad [5]$$

From where we can reorder the terms to obtain the following:

$$K_{d,1} = K_{d,2}\left(\frac{n_H}{2-n_H}\right)^2, \quad [6]$$

an expression that we can now use to directly relate the overall affinity of a two-site receptor—which, again, is given by the geometric mean of the affinities of its binding sites (Eq. **3**)—to its Hill coefficient:

$$K_{1/2} = \sqrt{K_{d,1}K_{d,2}} = K_{d,2}\frac{n_H}{2-n_H}. \quad [7]$$

Given these relationships, a two-site receptor achieving a Hill coefficient of 1.98 exhibits a dynamic range narrowed from the 81-fold seen in the absence of cooperativity to just 9.2-fold (Eq. **2**), but it does so at the expense of decreasing its overall affinity by at least a factor of 99 relative to that of its higher-affinity binding site (Eq. **7**, *SI Appendix*, Table S1, and Fig. 1).

The above arguments notwithstanding, the inherent trade-off between affinity and cooperativity can, in theory, be overcome by increasing the number of binding sites. Specifically, while the addition of more binding sites is generally thought of in terms of its ability to produce higher Hill coefficients, it should also be useful in improving affinity in scenarios in which less than maximal cooperativity is acceptable. For example, the overall affinity of a three-site receptor with a Hill coefficient of 1.98 need only be three times poorer than that of its highest-affinity binding site (Fig. 1*B* and *SI Appendix*). This contrasts sharply with the (at least) 99-fold reduction in affinity required in order for a two-site receptor to achieve an equivalent Hill coefficient.

Building on the above hypothesis, in this paper we describe an experimental demonstration of our ability to "tune" the trade-off between affinity and cooperativity in multisite receptors. To achieve this, we have rationally altered the binding energy landscape of a cooperative, three-site doxorubicin-targeting aptamer so as to tune the extent to which it partitions its binding energy between improved affinity and improved cooperativity. We selected this cancer chemotherapeutic as our target because it suffers from a narrow therapeutic window due to hepatic and cardiac toxicity. Given this, the higher precision measurements produced by a narrower dynamic range would be of significant clinical value, provided that the affinity of the receptor remains high enough to match the concentrations seen clinically.

Results

We have previously demonstrated an "intrinsic disorder" strategy by which we can rationally introduce cooperativity into normally uncooperative aptamers (11). This intrinsic disorder mechanism, which until then had only been described for heterotropic allosteric control of molecular recognition (20–22), has more recently been found to be employed by nature to generate cooperativity (homotropic allostery), such as the binding of calcium by the two intrinsically disordered domains of calmodulin (23) and the binding of the intrinsically disordered nuclear receptor corepressor (N-CoR) to the transcription factor retinoic acid receptor (RAR) (9). To achieve this effect by design, we split an aptamer into two halves, generated tandem repeats of each half, and then connected these via a flexible, unstructured loop. The first binding event requires closure of this loop, and thus its affinity is reduced by the entropy associated with the closure. The second binding event, in contrast, occurs after loop closure has "preformed" the second binding site, thus increasing its affinity as is required to induce cooperativity.

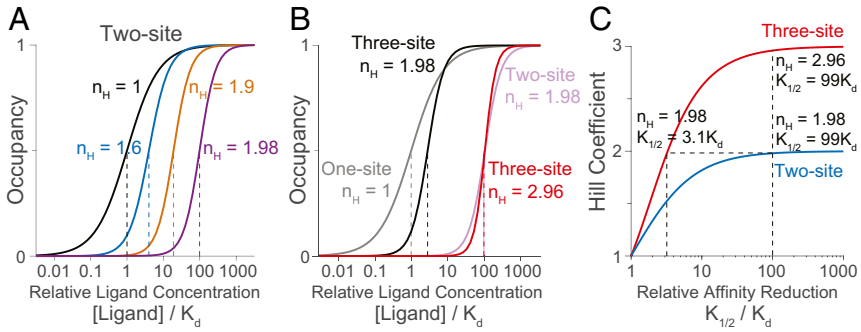

Fig. 1. Trade-off between cooperativity and affinity. Cooperativity improves a receptor's responsiveness to small changes in target concentration (i.e., increases the steepness of its binding curve, narrowing the dynamic range), but at the expense of reducing its affinity. (*A*) For example, the 9.2-fold dynamic range of a two-site cooperative receptor with a Hill coefficient (n_H) of 1.98 (in purple) is almost 9-fold narrower than that of its noncooperative parent receptor (black). This narrowing is achieved, however, at the cost of at least a 99-fold reduction in affinity ($K_{1/2}$) with respect to the maximum affinity of the noncooperative, parent receptor (K_d). (*B*) A cooperative receptor with three binding sites, in contrast, can achieve the same cooperativity (same n_H) as a two-site receptor while maintaining much higher affinity (black line). Alternatively, it can achieve a higher Hill coefficient (shown, in red, is a three-site receptor of $n_H = 2.96$) with the same loss of affinity seen for a less cooperative two-site receptor ($n_H = 1.98$, purple line). (*C*) A three-site receptor (red line) can thus achieve much higher cooperativity values, asymptotically approaching the maximum of $n_H = 3$, than a two-site receptor (blue line), whose maximum cooperativity is $n_H = 2$, or achieve the same degree of cooperativity without taking as great a "hit" in overall affinity.

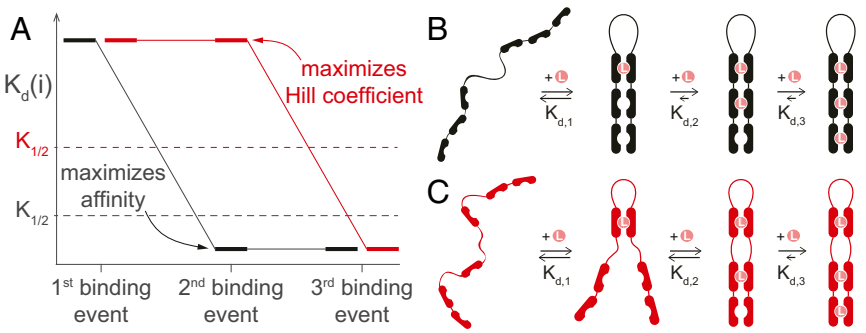

Fig. 2. The binding energy landscape determines the trade-off between cooperativity and overall affinity. (*A*) Here, we illustrate two (out of the many possible) binding energy landscapes for a three-site cooperative receptor. A landscape for which the increase in affinity occurs at the second binding event (black lines) produces near all-or-none binding at the second binding event, thus tilting the system toward lower cooperativity and higher affinity. Alternatively, a landscape for which the increase in affinity occurs at the third binding event (in red) produces near all-or-none binding at the third binding event, tilting the system toward greater cooperativity but poorer affinity. The affinity of the second binding event thus controls the trade-off between cooperativity and affinity. (*B*) To realize the former binding energy landscape, we introduce an unstructured loop that, upon closure, leads to the concerted formation of all three binding sites. This imposes an entropic penalty on the first binding event, which reduces its affinity relative to those of both subsequent binding events. (*C*) In contrast, a construct in which separate disordered loops must close to form the first and second binding sites reduces the affinity of the first two binding events relative to the third.

Using this approach, we have produced two-site cooperative aptamers binding cocaine and doxorubicin, the most cooperative of which achieves a Hill coefficient of 1.98 (11). Achieving the resulting near-9-fold narrowing of the dynamic range, however, comes at the cost of pushing the midpoint of the binding curve ~100-fold higher than that of the unmodified parent aptamer (Fig. 1 and *SI Appendix*, Table S1).

Building on our prior work, here we have explored the design of cooperative, three-site doxorubicin aptamers. To achieve a degree of cooperativity similar to that of the above-described, two-site aptamer while retaining better overall affinity, we first designed a three-site aptamer for which the affinity of its first binding event is poorer than that of its second and third (Fig. 2, black trace), thus producing the binding energy landscape predicted to maximize overall affinity. Conversely, to bias the landscape toward a higher Hill coefficient (at the cost of less than maximal affinity), we designed a second three-site aptamer for which the affinities of its first and second binding events are low and only that of its third is high (Fig. 2, red trace). This produces highly cooperative, "all-or-none" binding only upon the third binding event, thus achieving higher cooperativity than the previous energy landscape but at the cost of poorer overall affinity. Thus, we have based the design of our receptors on the idea that the affinity of the second binding event acts as a "gatekeeper," allosterically tuning the extent to which the energy provided by the third binding event is partitioned toward improving affinity or improving cooperativity.

To explore our strategy for improving affinity, we first designed doxorubicin-binding constructs containing one, two, or three half-site tandem repeats separated by a 30-thymine disordered loop (Fig. 2*B*). We modified each of these with an Alexa 488 fluorophore at the 5′ terminus and a BHQ1 quencher at the 3′ end, and then determined their cooperativity and overall affinity by performing doxorubicin titrations (Fig. 3 and *SI Appendix*, Table S2). As expected, the construct consisting of a single, loop-split binding site exhibits a Hill coefficient within error of unity ($n_H = 0.95 \pm 0.09$, reported uncertainties correspond to 95% confidence intervals derived from independent experimental replicates) and a $K_{1/2}$ some 7.5-fold poorer than that of the unmodified parent aptamer (*SI Appendix*, Fig. S1). The addition of a second binding site then introduces significant cooperativity ($n_H = 1.6 \pm 0.1$), but only at the cost of reducing the overall affinity by a factor of 3 relative to that of the parent aptamer. In contrast, the addition of a third binding site increases cooperativity slightly ($n_H = 1.9 \pm 0.1$) while simultaneously improving its affinity to within a factor of 2 of that of the parent aptamer, rendering its affinity at least 9-fold better than that of a two-site receptor achieving the same Hill coefficient (Fig. 1 and *SI Appendix*, Table S1).

While the addition of a second high-affinity binding site biases the landscape toward improved affinity, the addition of a second low-affinity binding site, in contrast, produces an energy landscape biased toward higher cooperativity (Fig. 2*A*). To design such a three-site aptamer, we employed a construct that introduces additional, unstructured loops between the first and second binding sites, reducing the affinity of the second binding event relative to that of the third (Fig. 2*C*). As expected, while the cooperativity of this construct is significantly enhanced ($n_H = 2.3 \pm 0.1$), its affinity

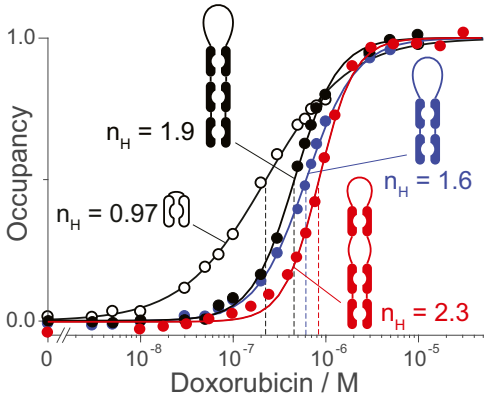

Fig. 3. Tuning the cooperativity–affinity trade-off in the doxorubicin aptamer. We have explored experimentally the trade-off between cooperativity and affinity by introducing various levels of cooperativity into a normally noncooperative doxorubicin-binding aptamer. The introduction of cooperativity always comes at a cost in affinity; compare, for example, the affinity of the noncooperative parent aptamer (open circles) with that of a cooperative, two-site aptamer (blue). The addition of a third binding site, however, provides an opportunity to tune this trade-off by regulating the extent to which the additional energy provided by the third binding event is partitioned between improving affinity or cooperativity. That is, depending on the details of its binding energy landscape, a three-site receptor can be tuned to achieve either high cooperativity at the cost of lower affinity (red), or somewhat lower cooperativity but with improved affinity (black).

is poorer (2-fold) than that of the less cooperative three-site construct (Fig. 3, red curve).

Experimental dissection of the binding energy landscapes of our constructs adds credence to our design strategies. To extract the individual affinities at each binding event, we fit our binding data to a Monod–Wyman–Changeux (MWC) model of three-site cooperative binding (see *SI Appendix* for a detailed description of the model). This model assumes that the affinity of each site is modulated by the energetic cost of closing its associated loops, and not by any differences in the intrinsic affinity of the three formed sites. Fitting the binding data of our three-site, single-loop construct to a MWC model requiring one switching event (*SI Appendix*, Fig. S2 and Eqs. S2–S5) produces a Hill coefficient and overall affinity within error of those derived via a fit to the empirical Hill equation (Table 1 and *SI Appendix*, Tables S2 and S3 and Fig. S4). The model also produces estimated individual affinities that reproduce the energy landscape expected to produce improved affinity (compare the black traces in Figs. 2 and 4), with the affinity of the "formed-upon-binding" first binding site being 20-fold poorer (equivalent to 7.5 ± 0.6 kJ·mol^{-1} less favorable binding energy) than that of the "preformed" second and third binding sites. Consistent with our design strategy, the affinities of the latter are within error of that of the parent aptamer (*SI Appendix*, Table S3). Following a similar approach, we have also characterized the binding energy landscape of the two-loop, three-site aptamer using a MWC model requiring two switching events to fully form all three binding sites (Table 1 and *SI Appendix*, Figs. S3 and S4, Table S3, and Eqs. S6–S9). As again expected, the affinities of the first and second binding events for this construct are poorer than that of the third (11 ± 1 kJ·mol^{-1} less favorable binding energy; *SI Appendix*, Table S3), thus producing the expected energy landscape biased toward cooperativity (compare the red traces in Figs. 2 and 4). Our results thus confirm that, by using intrinsic disorder to modulate the affinity of the second binding event, we can shape the binding energy landscape to rationally tune the trade-off between affinity and cooperativity.

Discussion

Here, we present a strategy to control the trade-off between the affinity and cooperativity of biomolecular receptors, which we have applied to the problem of rationally tuning the cooperativity and affinity of an aptamer. Specifically, we have shown that the extra binding energy provided by the addition of a third binding site to a previously described, two-site doxorubicin aptamer can be rationally partitioned between improving its cooperativity, its affinity, or both.

Nature selects biomolecular receptors with binding properties tailored to their specific functions. Cooperativity, for example, evolved in response to the need to increase the responsiveness of biomolecules to small changes in the concentration of their ligand. As it often happens, however, this improvement comes at an expense: poorer affinity. Here, we have investigated the thermodynamics underlying this trade-off by designing binding energy landscapes of controlled cooperativity and affinity. We find that, as predicated, the inclusion of additional binding sites can compensate for this trade-off by improving both cooperativity and affinity. We have likewise shown that the trade-off between the two is controlled by the relative affinities of these additional binding sites. Specifically, while the addition of high affinity binding sites maximizes overall affinity, the addition of low-affinity binding sites maximizes cooperativity and thus the responsiveness of the binding curve.

Given the modular nature of our design approach, and the generality of intrinsic disorder as a mechanism for allosteric control (20–22), we believe the strategies described here could be applicable to other systems for which the molecular recognition site can be separated in multiple domains. These include, for example, periplasmic binding proteins (24), DNA-binding peptides (25), and coiled-coil peptide motifs (26). Our work thus expands our ability to design cooperative receptors and tailor their affinity and cooperativity to, for example, support biotechnological applications such as biosensors (27), drug delivery (28), imaging (29), or biomolecule-based logic gates (30, 31).

Table 1. Tuning the trade-off between cooperativity and affinity for a three-site receptor

		Hill	MWC
Three-site, one-loop	n_H	1.9 ± 0.1	1.9 ± 0.1
	$K_{1/2}$, nM	460 ± 20	470 ± 30
	ΔG_b, kJ·mol^{-1}	−36.2 ± 0.2	−36.1 ± 0.3
Three-site, two-loops	n_H	2.3 ± 0.1	2.3 ± 0.1
	$K_{1/2}$, nM	860 ± 20	860 ± 20
	ΔG_b, kJ·mol^{-1}	−34.6 ± 0.1	−34.6 ± 0.1

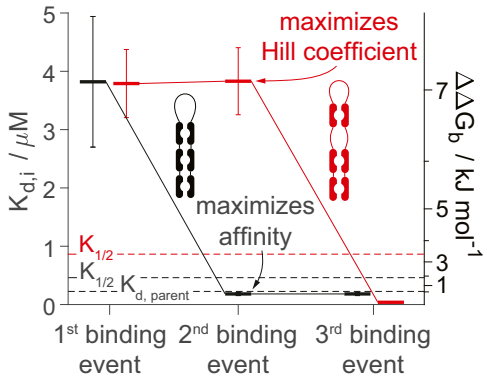

Fig. 4. Binding energy landscape for the described receptors. For our higher-affinity, lower-cooperativity construct (black trace), the affinity (*Left* axis) of the first binding event is much lower than those of the second and third, which are quite close to that of the parent aptamer, thus reproducing the binding energy landscape (*Right* axis) predicted to be biased toward affinity over cooperativity. In contrast, the energy landscape of our second, lower-affinity, higher-cooperativity construct features first and second binding events that are much lower in affinity than that of the third (red trace), biasing it toward cooperativity at the expense of affinity. Reported uncertainties correspond to 95% confidence intervals derived from experimental replicates.

Materials and Methods

Chemicals. Sodium chloride, sodium hydrogen phosphate, and potassium dihydrogen phosphate were ordered from Fisher Scientific. Doxorubicin hydrochloride was ordered from LC Laboratories. All chemicals were used as received.

Construct Design. The DNA constructs employed were purchased from IBA Lifesciences with an Alexa 488 fluorophore at the 5′ end and a black hole quencher (BHQ1) at the 3′ end. All were purified by high-performance liquid chromatography and mass verified by matrix-assisted laser desorption/ionization mass spectrometry. Their sequences were as follows: parent doxorubicin aptamer (28 nt), 5′-Alexa488-ACCATCTGTGTAAGGGGTAAGGGGTGGT-BHQ1-3′; one-binding site aptamer with 30-thymine loop (58 nt), 5′-Alexa488-ACCATCTGTGTAAGG-T_{30}-GGTAAGGGGTGGT-BHQ1-3′; two-binding site cooperative aptamer (86 nt), 5′-Alexa488-(ACCATCTGTGTAAGG)$_2$-T_{30}-(GGTAAGGGGTGGT)$_2$-BHQ1-3′; three-binding site cooperative aptamer with one loop (114 nt), 5′-Alexa488-(ACCATCTGTG-TAAGG)$_3$-T_{30}-(GGTAAGGGGTGGT)$_3$-BHQ1-3′; and three-binding site cooperative aptamer with two loops (114 nt), 5′-Alexa488-(ACCATCTGTGTAAGG)$_2$-T_7-ACCATCTGTGTAAGG-T_{15}-GGTAAGGGGTGGT-T_8-(GGTAAGGGGTGGT)$_2$-BHQ1-3′.

Doxorubicin Titrations Monitored by Fluorescence Spectroscopy. To determine the dissociation constants and Hill coefficients of our receptors, we performed doxorubicin titrations monitored by fluorescence spectroscopy. Specifically, we titrated 1 mL of 10 nM of the corresponding aptamer receptor construct in buffer 50 mM sodium phosphate (pH 7.0) at 37 °C with a stock

solution of doxorubicin hydrochloride. To monitor binding, we measured the quenching of the fluorescence of Alexa 488 by BHQ1 (excitation, 490 ± 5 nm; emission, 520 ± 5 nm) with a Varian Cary Eclipse fluorescence spectrophotometer. At each addition, we waited 1 min for mixing, measured the fluorescence kinetics for 3 min (to ensure that equilibration was effectively complete), and then reported the average of the last five points (corresponding to 1 min). To extract the apparent dissociation constants ($K_{1/2}$) and Hill coefficients (n_H), we fit the experimental data to the Hill equation using in house coded Matlab scripts:

$$F = \frac{F_{sat}[L]^{n_H} + F_0 K_{1/2}^{n_H}}{K_{1/2}^{n_H} + [L]^{n_H}} + m_{sat}[L], \quad [8]$$

where F are the fluorescence values measured as function of ligand concentration (L); F_0 and F_{sat}, the fluorescence values in the absence of ligand and at saturation; and m_{sat}, a linear baseline to account for the background fluorescence of doxorubicin (identical $K_{1/2}$ and n_H values were obtained by fitting the fluorescence corrected by the fluorescence of doxorubicin in buffer). For each titration, we measured at least three independent experimental replicates and reported uncertainties as the 95% confidence intervals.

Data Availability.

All materials, protocols, data, models, and parameters necessary to reproduce the work are reported in the main text and the associated *SI Appendix*. Raw fluorescence data is accessible in the GitHub public repository: https://github.com/gabodabo/Cooperativity-affinity-trade-off-PNAS2020.

ACKNOWLEDGMENTS. This work was funded by the NIH (Grant R01EB022015).

1. A. Goldbeter, On the role of enzyme cooperativity in metabolic oscillations: Analysis of the Hill coefficient in a model for glycolytic periodicities. *Biophys. Chem.* **6**, 95–99 (1976).
2. A. C. Notides, N. Lerner, D. E. Hamilton, Positive cooperativity of the estrogen receptor. *Proc. Natl. Acad. Sci. U.S.A.* **78**, 4926–4930 (1981).
3. H. Bisswanger, Cooperativity in highly aggregated enzyme systems. A slow transition model for the pyruvate dehydrogenase complex from *Escherichia coli*. *J. Biol. Chem.* **259**, 2457–2465 (1984).
4. D. E. Koshland Jr., K. Hamadani, Proteomics and models for enzyme cooperativity. *J. Biol. Chem.* **277**, 46841–46844 (2002).
5. S. Linse, W. J. Chazin, Quantitative measurements of the cooperativity in an EF-hand protein with sequential calcium binding. *Protein Sci.* **4**, 1038–1044 (1995).
6. T. Meyer, D. Holowka, L. Stryer, Highly cooperative opening of calcium channels by inositol 1,4,5-trisphosphate. *Science* **240**, 653–656 (1988).
7. F. Ferriere, N. A. Khan, J. P. Meyniel, P. Deschaux, Characterisation of serotonin transport mechanisms in rainbow trout peripheral blood lymphocytes: Role in PHA-induced lymphoproliferation. *Dev. Comp. Immunol.* **23**, 37–50 (1999).
8. T. Krell *et al*., Optimization of the palindromic order of the TtgR operator enhances binding cooperativity. *J. Mol. Biol.* **369**, 1188–1199 (2007).
9. T. N. Cordeiro *et al*., Interplay of protein disorder in retinoic acid receptor heterodimer and its corepressor regulates gene expression. *Structure* **27**, 1270–1285.e6 (2019).
10. A. Peselis, A. Gao, A. Serganov, Cooperativity, allostery and synergism in ligand binding to riboswitches. *Biochimie* **117**, 100–109 (2015).
11. A. J. Simon, A. Vallée-Bélisle, F. Ricci, K. W. Plaxco, Intrinsic disorder as a generalizable strategy for the rational design of highly responsive, allosterically cooperative receptors. *Proc. Natl. Acad. Sci. U.S.A.* **111**, 15048–15053 (2014).
12. A. J. Simon, A. Vallée-Bélisle, F. Ricci, H. M. Watkins, K. W. Plaxco, Using the population-shift mechanism to rationally introduce "Hill-type" cooperativity into a normally non-cooperative receptor. *Angew. Chem. Int. Ed. Engl.* **53**, 9471–9475 (2014).
13. N. Zandany, M. Ovadia, I. Orr, O. Yifrach, Direct analysis of cooperativity in multisubunit allosteric proteins. *Proc. Natl. Acad. Sci. U.S.A.* **105**, 11697–11702 (2008).
14. D. Mariottini, A. Idili, A. Vallée-Bélisle, K. W. Plaxco, F. Ricci, A DNA nanodevice that loads and releases a cargo with hemoglobin-like allosteric control and cooperativity. *Nano Lett.* **17**, 3225–3230 (2017).
15. A. V. Hill, The possible effects of the aggregation of the molecules of hemoglobin on its dissociation curves. *J. Physiol.* **40**, iv–vii (1910).
16. J. Monod, J. Wyman, J.-P. Changeux, On the nature of allosteric transitions: A plausible model. *J. Mol. Biol.* **12**, 88–118 (1965).
17. L. Pauling, The oxygen equilibrium of hemoglobin and its structural interpretation. *Proc. Natl. Acad. Sci. U.S.A.* **21**, 186–191 (1935).
18. W. Lenz, Beitrag zum Verständnis der magnetischen Erscheinungen in festen Körpern. *Phys. Z.* **21**, 613–615 (1920).
19. F. W. Dahlquist, The meaning of Scatchard and Hill plots. *Methods Enzymol.* **48**, 270–299 (1978).
20. V. J. Hilser, E. B. Thompson, Intrinsic disorder as a mechanism to optimize allosteric coupling in proteins. *Proc. Natl. Acad. Sci. U.S.A.* **104**, 8311–8315 (2007).
21. A. C. Ferreon, J. C. Ferreon, P. E. Wright, A. A. Deniz, Modulation of allostery by protein intrinsic disorder. *Nature* **498**, 390–394 (2013).
22. H. N. Motlagh, J. O. Wrabl, J. Li, V. J. Hilser, The ensemble nature of allostery. *Nature* **508**, 331–339 (2014).
23. G. Bernardo-Seisdedos *et al*., Structural basis and energy landscape for the Ca^{2+} gating and calmodulation of the Kv7.2 K^+ channel. *Proc. Natl. Acad. Sci. U.S.A.* **115**, 2395–2400 (2018).
24. G. Ortega, D. Castaño, T. Diercks, O. Millet, Carbohydrate affinity for the glucose-galactose binding protein is regulated by allosteric domain motions. *J. Am. Chem. Soc.* **134**, 19869–19876 (2012).
25. M. E. Vázquez, A. M. Caamaño, J. L. Mascareñas, From transcription factors to designed sequence-specific DNA-binding peptides. *Chem. Soc. Rev.* **32**, 338–349 (2003).
26. C. Mueller, T. N. Grossmann, Coiled-coil peptide beacon: A tunable conformational switch for protein detection. *Angew. Chem. Int. Ed. Engl.* **57**, 17079–17083 (2018).
27. H. Yu, J. Canoura, B. Guntupalli, X. Lou, Y. Xiao, A cooperative-binding split aptamer assay for rapid, specific and ultra-sensitive fluorescence detection of cocaine in saliva. *Chem. Sci.* **8**, 131–141 (2017).
28. Y. Li, Y. Wang, G. Huang, J. Gao, Cooperativity principles in self-assembled nanomedicine. *Chem. Rev.* **118**, 5359–5391 (2018).
29. Y. Li *et al*., Molecular basis of cooperativity in pH-triggered supramolecular self-assembly. *Nat. Commun.* **7**, 13214 (2016).
30. J. Bonnet, P. Yin, M. E. Ortiz, P. Subsoontorn, D. Endy, Amplifying genetic logic gates. *Science* **340**, 599–603 (2013).
31. B. Shlyahovsky, Y. Li, O. Lioubashevski, J. Elbaz, I. Willner, Logic gates and antisense DNA devices operating on a translator nucleic acid scaffold. *ACS Nano* **3**, 1831–1843 (2009).